

Comparison of influence of nanomaterials on a glassy carbon paste electrode-based bioanode in biofuel cells

Sema ASLAN, Murat TUTUM, Yudum TEPELİ, Ülkü ANIK*

Department of Chemistry, Faculty of Science, Muğla Sıtkı Koçman University, Kötekli, Muğla, Turkey

Received: 30.12.2015

Accepted/Published Online: 21.03.2016

Final Version: 02.11.2016

Abstract: This paper presents a comparative study of nanomaterial modified glassy carbon paste electrodes (GCPEs) used as bioanodes in enzymatic biofuel cells. The developed bioanode electrodes were obtained by modification of composite GCPEs with glucose oxidase (GOx) and different nanomaterials like manganese(IV) oxide nanoparticle (MnO_2 np) and aluminum titanate ($\text{Al}_2\text{O}_3\text{-TiO}_2$) bimetallic nanostructure. These nanostructures were utilized in a GCPE-based enzymatic bioanode construction for the first time. P-benzoquinone mediator was used for the electron transfer between enzyme redox center and bioanode electrode where glucose analyte was used as substrate. A laccase-modified plain GCPE was used as biocathode electrode. Then these electrodes were combined in a membraneless biofuel cell (BFC). The power densities of single cell BFCs were $0.619 \mu\text{W cm}^{-2}$ (at 34 mV) for the plain GCPE, $4.57 \mu\text{W cm}^{-2}$ (at 76 mV) for the GOx/ MnO_2 np/GCPE, and $1.41 \mu\text{W cm}^{-2}$ (at 36 mV) for the GOx/ $\text{Al}_2\text{O}_3\text{-TiO}_2$ /GCPE. As a result, it has been observed that the MnO_2 np/GOx/GCPE exhibits the best power density. The current density value of this bioanode has also been examined and found to be $99.21 \mu\text{A cm}^{-2}$ in phosphate buffer solution (pH 7) with maximum open circuit potential of 294 mV.

Key words: Enzymatic biofuel cell, manganese(IV) oxide nanoparticles, aluminum titanate bimetallic nanostructure, glassy carbon paste electrode

1. Introduction

Enzymatic biofuel cells (BFCs) can be described as systems that convert the chemical energy of specific substrates to electrical energy where enzymes act as catalysts. It has been shown that certain enzymes possess highly favorable catalytic properties in comparison to inorganic catalysts as they are renewable and noncorrosive. Moreover, enzymatic BFCs attract much attention in the implantable devices area since they can be operated in mild conditions such as at neutral pH values.¹⁻³

Quinones are very popular neutral mediators and utilize electron transport in the form of ubiquinones, which are electron acceptors for flavoproteins in the respiratory chain.⁴ There are several enzymatic studies that used benzoquinone (BQ) as mediator in enzymatic reactions.⁵⁻⁸ On the other hand, in order to obtain high power output and develop the performance of BFCs, nanomaterials have been widely used in the fabrication of these systems.

Graphene oxide and graphene-platinum hybrid nanoparticles, gold and cobalt oxide nanoparticles, and functionalized carbon nanotubes are examples of nanomaterials that have been used in BFCs.⁹⁻¹⁴ In this work,

*Correspondence: ulkuanik@gmail.com

manganese(IV) oxide nanoparticle (MnO_2 np) and aluminum titanate ($\text{Al}_2\text{O}_3\text{-TiO}_2$) bimetallic nanostructures were used with a glassy carbon paste electrode (GCPE) separately in the preparation of bioanodes.

As a nanomaterial, MnO_2 nps exhibit unique electrocatalytic properties when they are incorporated into the electrode structure. These nanoparticles are especially important for decomposition of H_2O_2 because they show excellent electrocatalytic activity during this process. It has also been demonstrated that use of MnO_2 np provides better sensitivity compared to a bare GCPE for ascorbic acid detection.¹⁵ Thus, various MnO_2 np modified electrodes were utilized in electroanalytical applications for H_2O_2 monitoring or for lactate and ascorbic acid detection.^{16–24}

On the other hand, there is one work in the literature that covers the usage of $\text{Al}_2\text{O}_3\text{-TiO}_2$ nanopowder as glutathione (GSH) biosensor and it was reported by our group. In that work, $\text{Al}_2\text{O}_3\text{-TiO}_2$ nanopowder and gold nanoparticle were used to modify a GCPE and used for GSH detection in wine and human urine samples. $\text{Al}_2\text{O}_3\text{-TiO}_2$ nanopowder addition to the electrode structure provided high stability and enhanced the sensitivity of the biosensor.²⁵

Considering the GCPE, there are many works in the literature, especially done by our group, that cover the usage of this electrode as biosensor transducer.^{8,15,25} Since MnO_2 np and $\text{Al}_2\text{O}_3\text{-TiO}_2$ nanostructures exhibit sensitive and stable results when used in biosensors, we think that their performance in BFCs is worth examining. As far as we know, $\text{Al}_2\text{O}_3\text{-TiO}_2$ nanostructures have never been used in BFC construction before; additionally this is the first study where MnO_2 np and $\text{Al}_2\text{O}_3\text{-TiO}_2$ nanostructures were used as modifiers for composite bioanodes. Bioanode electrodes were obtained by modification of a GCPE with glucose oxidase (GOx) and nanomaterials like MnO_2 np and $\text{Al}_2\text{O}_3\text{-TiO}_2$. p-BQ was used as mediator. The developed bioanodes were combined with laccase (Lac)-modified plain GCPE biocathodes and a membraneless single cell BFC was formed. The maximum open circuit potential (OCP) and power and current density outputs of the developed BFCs were measured and compared.

2. Results and discussion

2.1. Characterization of synthesized MnO_2 np

Since $\text{Al}_2\text{O}_3\text{-TiO}_2$ nanostructures were commercially available, only the characterization of the synthesized MnO_2 nps was performed. For this purpose, a TEM image of the synthesized MnO_2 np was provided and is presented in Figure 1. As can be seen from the TEM results, MnO_2 nps were formed in clusters. However, these clusters' shape is in accordance with our previous study and also similar studies that include these nanoparticles.^{26–28}

2.2. Electrochemical characterization of the developed bioanodes

The aim of the present study was to observe the effect of various nanomaterials on the performance of the developed BFCs. However, before investigating their performance in BFCs, MnO_2 np and $\text{Al}_2\text{O}_3\text{-TiO}_2$ nanostructure modified GOx/GCPE bioanodes' electrochemical performance was examined by using linear sweep voltammetry (LSV). Measurements were recorded between -0.2 and 1.2 V at a scan rate of 10 mV s⁻¹ with nanostructure-free and modified GOx/GCPE electrodes in 20 mM BQ and 250 mM glucose containing 10 mL of 100 mM PBS. A comparison of the voltammograms is given in Figure 2. The current values were obtained as 226.00 μA for the nanoparticle-free GOx/GCPE, 249.17 μA for the GOx/ $\text{Al}_2\text{O}_3\text{-TiO}_2$ /GCPE, and 427.00 μA for the GOx/ MnO_2 np/GCPE. Based on these results, it can be said that the best bioanode system is the GOx/ MnO_2 np/GCPE.

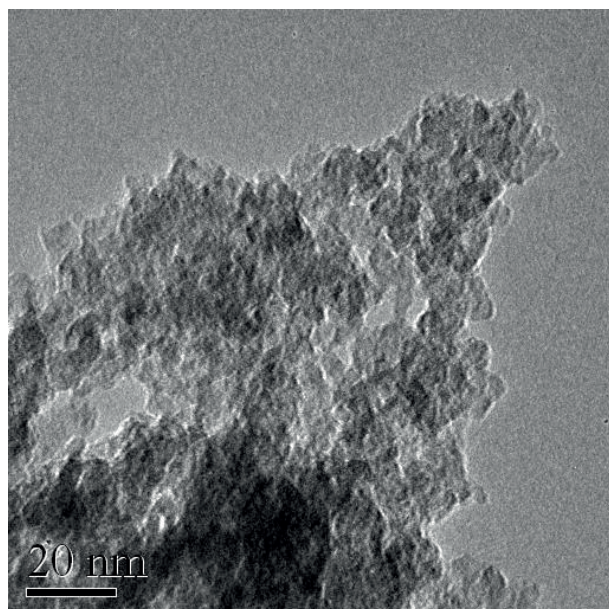


Figure 1. TEM image of synthesized MnO_2 np.

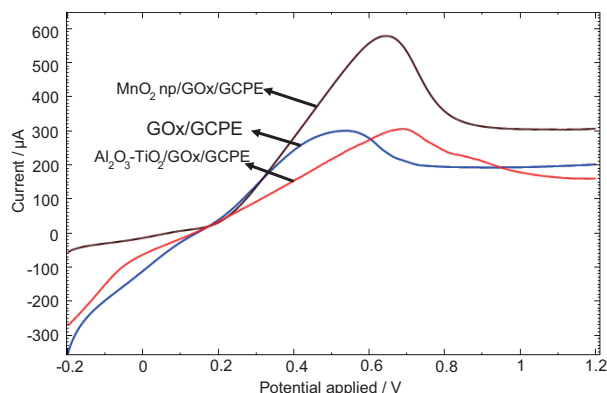


Figure 2. Comparison of voltammograms obtained from plain and nanomaterial modified GCPEs at optimum conditions where LSV was applied between -0.2 and 1.2 V with a scan rate of 10 mV s^{-1} .

After the electrochemical characterization studies, bioanodes and biocathodes with optimum enzyme amounts were combined in a single cell enzymatic BFC and the measurements were recorded under optimum operating conditions that were reported in our previous study.⁸ These conditions are also given in Table 1.

Table 1. Optimum experimental parameters.⁸

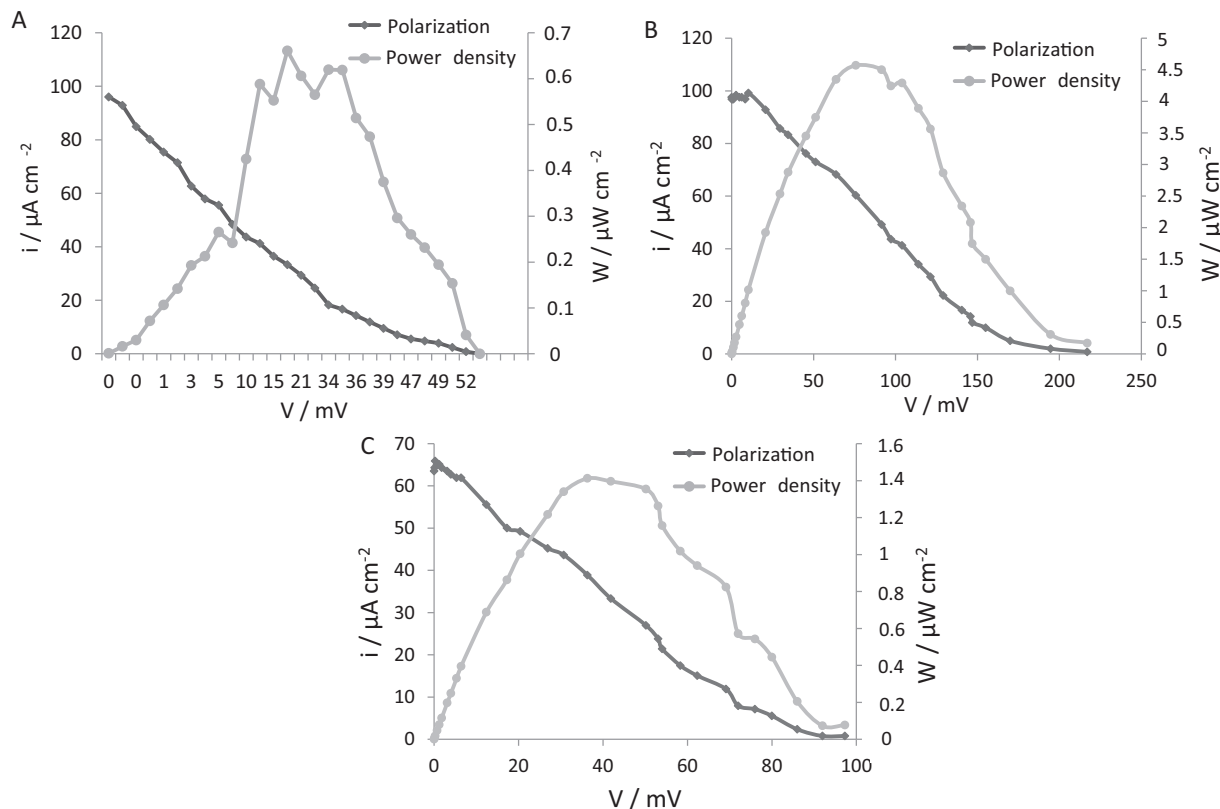
Experimental parameters	Optimum values
GOx amount	55.7 unit
Lac amount	25.2 unit
BQ concentration	20 mM
Phosphate buffer solution concentration	100 mM
Optimum pH	7

2.3. Polarization and power measurements

The GOx/GCPE, GOx/ MnO_2 np/GCPE, and GOx/ Al_2O_3 - TiO_2 /GCPE bioanodes were combined with the Lac/GCPE biocathode in a membraneless single cell BFC and current/voltage measurements were recorded using a multimeter. Polarization and power measurements were performed and calculated as explained in the instruments and measurements section. The polarization and power curves of the plain (nanoparticle-free) GOx/GCPE bioanode based BFC are presented in Figure 3A; the same curves for the GOx/ MnO_2 np/GCPE bioanode-based BFC and the GOx/ Al_2O_3 - TiO_2 /GCPE bioanode-based BFC are presented in Figures 3B and 3C, respectively. Maximum power density, maximum current density, and maximum OCP values of all BFC systems are presented in Table 2.

Table 2. Maximum power density, maximum current density, and maximum OCP values of all single cell BFC systems.

Bioanodes	OCP/mV	Maximum current	Maximum power
		density/ $\mu\text{A cm}^{-2}$	density/ $\mu\text{W cm}^{-2}$
GOx/GCPE	117	96.03	0.619 (34 mV)
GOx/MnO ₂ np/GCPE	294	99.21	4.57 (76 mV)
GOx/Al ₂ O ₃ -TiO ₂ /GCPE	115	65.87	1.41 (36 mV)

**Figure 3.** Polarization and power curves of A) plain (nanoparticle free) GOx/GCPE bioanode, B) GOx/MnO₂ np/GCPE bioanode, C) GOx/Al₂O₃-TiO₂/GCPE bioanode based single cell BFCs.

As can be clearly seen from Table 2, the GOx/MnO₂ np/GCPE bioanode-based BFC in Figure 3B gives the best results. This is attributed to the contribution of the electrochemical catalytic property of MnO₂ np with enzyme and GCPE in the bioanode structure. Attributed electrocatalytic effects of MnO₂ nps are not new. Çevik et al. and Luo et al. also reported that the use of MnO₂ np provides better sensitivity compared to bare electrodes for ascorbic acid detection and for glucose biosensors.^{15,19}

Overall, in the above studies, it has been demonstrated that the better results obtained were due to MnO₂ np introduced in the electrodes' structures.^{15,19} On the other hand, the GOx/Al₂O₃-TiO₂/GCPE bioanode exhibited lower maximum current and power densities compared to the GOx/MnO₂ np/GCPE bioanode. If the GOx/GCPE bioanode's performance is compared with that of the GOx/Al₂O₃-TiO₂/GCPE bioanode, it can be seen that the GOx/Al₂O₃-TiO₂/GCPE bioanode showed better power density but lower maximum current density and OCP values (Table 2).

2.4. OCP measurements of the developed BFCs

Obtaining higher OCP values from the BFCs is an important point because of the dependence between obtaining sufficient high voltages for long-term usage of the BFCs. For example, OCP value is very important for the case of electronic power supply of implantable electronic devices.²⁹ Thus we measured OCP values of the developed BFCs while there was no current flow in the system. OCP values of three different single cell BFCs were recorded for 24 h by multimeter in a 10-mL cell. At the first stages of the measurements, OCP values increased up to a certain point, then decreased, and stayed at a steady state value for approximately 2 h. The $\text{Al}_2\text{O}_3\text{-TiO}_2$ modified bioanode did not show any OCP value after 5 h. The maximum OCP value was observed as 294 mV with the GOx/MnO_2 np/GCPE used BFC. OCP values of each system are shown in Table 2 and time vs. OCP curves of the developed BFCs are compared in Figure 4. Measurements were recorded for 24 h but since significant differences were observed after 6 h, Figure 4 demonstrates only 6 h measurements.

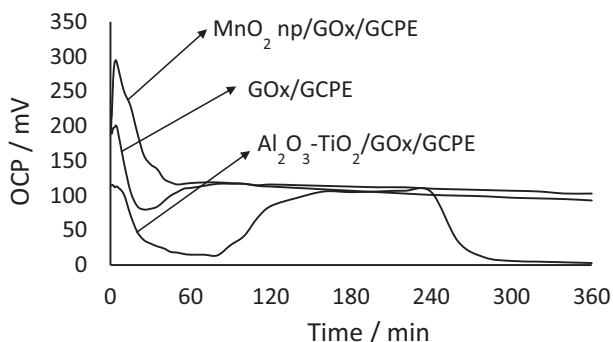


Figure 4. OCP measurements of single cell BFCs (OCP vs. time for 6 h).

2.5. Reproducibility values and storage stability

Since better results were obtained with the GOx/MnO_2 np/GCPE compared with the GOx/Al-TiO_2 /GCPE, reproducibility values and storage stability studies were conducted for this electrode. The RSD values of bioanode and biocathode were calculated as 5.91% and 7.88%, respectively, by using LSV. In terms of storage stability, there was a current loss of 7.30% between the first and seventh day of the GOx/MnO_2 np/GCPE bioanode.

2.6. Comparison of performance of similar BFC studies

The developed BFC system was compared with similar BFC systems as shown in Table 3. Kiliç et al. reported an enzymatic BFC with various mediators such as ferrocene, neutral red, and p-benzoquinone modified polypyrrole-2-carboxylic acid for the oxidation of glucose in domestic wastewater. In that study, glucose in domestic wastewater was utilized for energy generation. The maximum power density (given in Table 3) was observed for the ferrocene-modified electrodes including GOx and Lac as anodic and cathodic enzymes, respectively.³⁰ Furthermore, du Toit et al. demonstrated two different continuous flow-through enzymatic biofuel cells (CFEBFCs) without redox mediators in the presence of GOx at the highly porous gold (hPG) anode and Lac at the hPG biocathode. In the first design, the anode and the cathode were integrated in two parallel channels separated by a PDMS wall. In the second design there was a single channel containing those two electrodes. The observed maximum current and power outputs of these two designs were also lower than those in the present study as given in Table 3.³¹ Similarly, Kim et al. developed an enzymatic fuel cell that used

a high-quality graphite oxide/Co composite as mediator system where self-assembled GOx and Lac were used as the anode biocatalyst and cathode biocatalyst, respectively, on Au electrodes.³² In that study, the power and OCP values were again lower than those of our BFCs. In addition, single cell and mediatorless enzymatic BFCs were reported by Wang et al.³³ In that study, they deposited single wall carbon nanotubes (SWNTs) on porous silicon (pSi) substrates by two different methods. Subsequently GOx and Lac were immobilized on the pSi/SWNT substrates to obtain bioanode and biocathode and then combined as BFCs in pH 7 phosphate buffer solution. As can be seen clearly from Table 3, the obtained results were lower than our values.

Table 3. Comparison of the performances of similar BFC studies

Bioanode and biocathode	Mediator	Maximum current density/ $\mu\text{W cm}^{-2}$	Maximum power density/ $\mu\text{W cm}^{-2}$	OCP/mV	Reference
Polypyrrole-2-carboxylic acid/GOx and Lac	Ferrocene	-	1	-	30
hPG/GOx and hPG/Lac parallel channel CFEBFCs	-	< 20	1.6	< 350	31
hPG/GOx and hPG/Lac single channel CFEBFCs	-	< 15	0.7	250	31
Au-GOx and Au-Lac	Cobalt	-	1.058	578	32
pSi/SWNT/GOx and pSi/SWNT/Lac	-	< 30	1.38	-	33
GOx/MnO ₂ np/GCPE and Lac/GCPE	BQ	294	99.21	4.57	Present study

Here three different bioanodes, the GOx/GCPE, GOx/Al₂O₃-TiO₂/GCPE, and GOx/MnO₂ np/GCPE, were prepared. The performance of these bioanodes was compared by combining them with Lac/GCPE biocathode and forming a single cell BFC. Among them, the GOx/MnO₂ np/GCPE provides the best power density and OCP value by facilitating electron transfer kinetics. When the GOx/MnO₂ np/GCPE-based bioanode BFC was compared with similar BFCs, it is observed that our system provided better output values. Considering the composite nature of the GCPE, which brings practicality and makes the BFC economical, we can conclude that a robust, practical, and economical BFC system has been produced.

3. Experimental

3.1. Chemical reagents

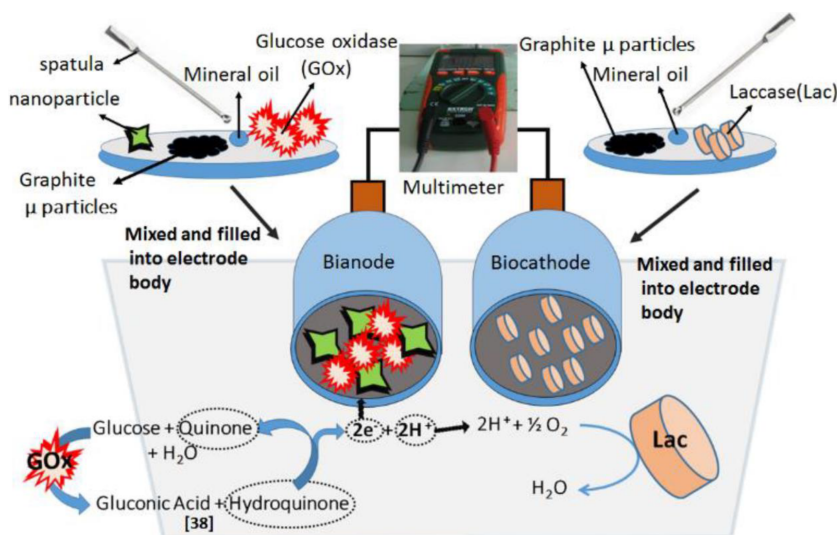
Phosphate buffer solution was prepared from KH₂PO₄ (99.995% pure, Merck) and used as anolyte; acetate buffer solution was prepared from CH₃COOH (100% pure, Merck) and used as catholyte. For pH adjustments of buffer solutions 1 M NaOH (97% pure, Merck) was used. GOx (from *Aspergillus niger*, Sigma) enzyme was used for bioanode preparation. Glucose monohydrate D(+) (Merck) was used as substrate, BQ (98% pure, Merck) as mediator. Lac (from *Trametes versicolor*, 21 U/mg, Sigma) enzyme was used in the biocathode fabrication. The Al₂O₃-TiO₂ bimetallic nanostructure was purchased from Sigma (nanopowder < 25 nm (BET) 98.5%, Sigma). MnO₂ np was prepared in our laboratory as reported before.¹⁹ Glassy carbon, spherical powder (2–12 μm , Merck), and mineral oil (Sigma-Aldrich) were used in the preparation of the GCPEs.

3.2. Instruments and measurements

Electrochemical measurements of the developed electrodes were monitored by AUTOLAB PGSTAT 12 and μ -AUTOLAB TYPE III potentiostat/galvanostat by LSV. Measurements were carried out in a standard three-electrode cell containing a platinum wire auxiliary electrode, a Ag|AgCl ((Ag/AgCl/KCl (1 M)) (filled with 1 M KCl, Metrohm) reference electrode, and modified GCPEs as working electrodes. The electrodes were inserted into a conventional electrochemical cell. Optimization of temperature and pH parameters of the bioanode were monitored by LSV between -0.2 and 1.2 V at a scan rate of 10 mV s^{-1} with the GOx/GCPE electrode in 20 mM BQ and 250 mM glucose and 10 mL of 100 mM PBS . Current/voltage measurements of the BFC was conducted with an Autoranging Mini Multimeter (MN16A) equipped for current and voltage measurements of developed enzymatic BFCs. Current (I) values of the BFC were measured while different external resistances (R) (from 1Ω to $10 \text{ M}\Omega$) were inserted to the circuit in order to calculate cell voltage (V_{cell}) ($V_{\text{cell}} = IR$) and power (P) ($P = V_{\text{cell}}I$). The current density (i) ($i = IA^{-1}$) and power density (W) ($W = PA^{-1}$) values were obtained by dividing current and power values by the surface area of the electrode ($A = 0.126 \text{ cm}^2$). TEM images were recorded using a JEOL-JEM 2100.

3.3. Preparation of electrodes and fabrication of BFCs

GCPE-based bioanodes and biocathode were prepared by mixing appropriate amounts of glassy carbon microparticle, mineral oil, desired enzyme (ratios for bioanode glassy carbon microparticle:GOx:mineral oil as $66:14:20\% \text{ w w}^{-1}$ and ratios for biocathode glassy carbon micro particle:Lac:mineral oil as $65:15:20\% \text{ w w}^{-1}$). Optimum amounts of desired nanoparticles were also added to the paste for bioanode fabrication ($2 \mu\text{L}$ of MnO_2 np and ratios of glassy carbon microparticle:GOx:mineral oil: Al_2O_3 - TiO_2 nanopowder as $46:14:20:20$ ($\% \text{ w w}^{-1}$). Then the resulting paste mixture was placed into the hole (2 mm radius, 3 mm deep) on a Delrin body where a copper wire provides the electrochemical connection. The surface of the electrode was polished on plain paper before every measurement. These electrodes were connected to a multimeter and dipped into a 10-mL cell that contained 20 mM BQ ($\text{pH } 7$). By this way, a single cell BFC system was fabricated where glucose was used as substrate (Scheme).



Scheme. Illustration of composite bioanode and biocathode electrode preparation and combination of enzymatic BFC system.

References

1. Kim, H. H.; Mano, N.; Zhang, Y.; Heller, A. *J. Electrochem. Soc.* **2003**, *150*, A209-A213.
2. Heller, A. *Phys. Chem. Chem. Phys.* **2004**, *6*, 209-216.
3. Bunte, C.; Hussein, L.; Gerald, A. *J. Power Sour.* **2014**, *247*, 579-586.
4. Murthy, A. S. N.; Sharma, J. *P Indian as-Chem Sci.* **1997**, *109*, 295-301.
5. Ikeda, T.; Katasho, I.; Kamei, M.; Senda, M. *Agr. Biol. Chem. Tokyo* **1984**, *48*, 1969-1976.
6. Ikeda, T.; Hamada, H.; Miki, K.; Senda, M. *Agr. Biol. Chem. Tokyo* **1985**, *49*, 541-543.
7. Li, J.; Yu, Y.; Wang, Y.; Qian, J.; Zhi, J. *Electrochim. Acta* **2013**, *97*, 52-57.
8. Anik, U.; Tutum, M.; Aslan, S. *Curr. Anal. Chem.* **2016**, *12*, 54-59.
9. Liu, C.; Alwarappan, S.; Chen, Z.; Kong, X.; Li, C. Z. *Biosens. Bioelectron.* **2010**, *25*, 1829-1833.
10. Li, Y.; Tang, L.; Li, J. *Electrochem. Commun.* **2009**, *11*, 846-849.
11. Najafabadi, A. T.; Ng, N.; Gyenge, E. *Biosens. Bioelectron.* **2016**, *81*, 103-110.
12. Chen, Y.; Gai, P.; Xue, J. J.; Zhang, J. R.; Zhu, J. J. *Biosens. Bioelectron.* **2015**, *74*, 142-149.
13. Kilic, M. S.; Korkut, S.; Hazer, B.; Erhan, E. *Biosens. Bioelectron.* **2014**, *61*, 500-505.
14. Arrocha, A. A.; Castillo, U. C. Aguila, S. A.; Duhalt, R. V. *Biosens. Bioelectron.* **2014**, *61*, 569-574.
15. Çevik, S.; Akpolat, O.; Anik, Ü. *Food Anal. Method.* **2016**, *9*, 500-504.
16. Yao, S.; Xu, J.; Wang, Y.; Chen, X.; Xu, Y.; Hu, S. *Anal. Chim. Acta* **2006**, *557*, 78-84.
17. Hocevar, S. B.; Ogorevc, B.; Schachl, K.; Kalcher, K. *Electroanal.* **2004**, *16*, 1711-1716.
18. Lin, Y.; Cui, X.; Li, L. *Electrochem. Commun.* **2005**, *7*, 166-172.
19. Luo, X. L.; Xu, J. J.; Zhao, W.; Chen, H. Y. *Biosens. Bioelectron.* **2004**, *19*, 1295-1300.
20. Yao, S.; Xu, J.; Wang, Y.; Chen, X.; Xu, Y.; Hu, S. *Anal. Chim. Acta* **2006**, *557*, 78-84.
21. Hocevar, S. B.; Ogorevc, B.; Schachl, K.; Kalcher, K. *Electroanal.* **2004**, *16*, 1711-1716.
22. Lin, Y.; Cui, X.; Liyu, L. *Electrochem. Commun.* **2005**, *7*, 166-172.
23. Xu, J. J.; Zhao, W.; Luo, X. L.; Chen, H. Y. *Chem. Commun.* **2005**, *3*, 792-794.
24. Williams, D. L.; Doig, A. R.; Korosi, A. *Anal. Chem.* **1970**, *42*, 118-121.
25. Çubukçu, M.; Ertas, F. N.; Anik, Ü. *Curr. Anal. Chem.* **2012**, *8*, 351-357.
26. Aslan, S.; Yavuz, Y.; Anik, Ü. *Curr. Anal. Chem.* **2014**, *10*, 435-442.
27. Yu, J.; Zhao, T.; Zeng, B. *Electrochem. Commun.* **2008**, *10*, 1318-1321.
28. Billik, P.; Čaplovičová, M.; Janata, J.; Fajnor, V.Š. *Mater. Lett.* **2008**, *62*, 1052-1054.
29. Zebda, A.; Gondran, C.; Le Goff, A.; Holzinger, M.; Cinquin, P.; Cosnier, S. *Nat. Commun.* **2011**, *2*:370 doi: 10.1038/ncomms1365.
30. Kiliç, M. S.; Korkut, S.; Hazer, B. In *Environmental Impact II*; Passerini G.; Brebbia, C. A., Eds. WIT Transactions on Ecology and the Environment: Ashurst Lodge, Ashurst, Southampton, UK, 2014, pp. 213-224.
31. du Toit, H.; Di Lorenzo, M. *Biosens. Bioelectron.* **2015**, *69*, 199-205.
32. Kim, D. S.; Kim, S. B.; Yang, X.; Lee, J. H.; Yoo, H. Y.; Chun, Y.; Cho, J.; Park, C.; Lee, J.; Kim S. W. *J. Electrochem. Soc.* **2015**, *162*, G113-G118.
33. Wang, S. C.; Yang, F.; Silva, M.; Zarow, A.; Wang, Y.; Iqbal Z. *Electrochem. Commun.* **2009**, *11*, 34-37.